First-order quantum phase transition in an anisotropic Ising model with infinite-range random interaction

J. Roberto Viana,[1] Angsula Ghosh,[1] and J. Ricardo de Sousa[1,2]
[1]*Departamento de Física, Universidade Federal do Amazonas, 3000, Japiim, 69077-000, Manaus-AM, Brazil*
[2]*Departamento de Física, ICEx, Universidade Federal de Minas Gerais, Av. Antônio Carlos 6627, CP 702, 30123-970, Belo Horizonte-MG, Brazil*
(Received 11 September 2007; published 23 January 2008)

The phase diagram of the spin 1 quantum van Hemmen spin glass model with biaxial crystal-field anisotropy and a transverse magnetic field is studied. We investigate the effects of the two transverse crystal-field parameters (D_x and D_y) and transverse field (Ω) on the phase diagrams in the $T-D_x$ plane for various values of D_y and Ω. Tricritical and reentrant behavior can be seen for appropriate ranges of these parameters.

DOI: 10.1103/PhysRevB.77.024424 PACS number(s): 05.70.−a, 75.10.Nr, 75.50.Lk, 64.60.−i

I. INTRODUCTION

Recently, the study of quantum phase transition is a topic of great interest in condensed matter and statistical physics,[1–3] especially due to the availability of various experimental results, for example: the quantum spin glass $LiHo_xY_{1-x}F_4$,[4] two-dimensional electron gas in semiconductor heterostructures,[5] heavy fermion material $CeCu_{6-x}Au_x$,[6] high-temperature superconductors,[7] etc. Systems near criticality are usually characterized by fluctuations over many length scales. In contrast to the phase transitions in classical models, quantum systems have fluctuations driven by the Heisenberg uncertainty principle even in the ground state. The analysis of the ground state and its thermodynamic properties are thus of central importance for understanding the critical behavior of such systems.

The quantum phase transition is governed by quantum fluctuations, and appears in the vicinity of zero temperature when an external parameter is varied. These quantum fluctuations may permit the system to pass from one local minimum of the free energy to another due to tunneling through barrier at rates that do not vanish as temperature T approaches zero. The statics and the dynamics are inextricably linked. Another interesting subject is that the thermal physics (classical phase transition) is inherently dissipative, while the quantum phase transition ($T=0$) is governed by the Schrödinger equation where energy is conserved and does not depend on time.

On the other hand, in the presence of disorder one encounters new features that are usually absent in the pure system. The random competition between ferromagnetic and antiferromagnetic interactions, although this competition may have a number of possible microscopic states, is the necessary requirement for the existence of the spin glass (SG) phase. The SG phase has been observed in various physical systems; e.g., in the metallic alloys with substitutional magnetic impurities such as CuMn and AuFe. Other examples are the amorphous systems and in compounds with nonequivalent sites randomly available to magnetic ions.

From the theoretical point of view, the study of the SG phase represents a quite difficult task in statistical mechanics. In the literature, the SG theory has been based on infinite-range interactions models, that are exactly solvable, and give a first qualitative understanding of the thermodynamical behavior. Among them are the susceptibility *cusp* at the freezing temperature and the field induced transition away from SG phase at finite magnetic field. The model proposed years ago by Sherrington and Kirkpatrick (SK),[8] denoted by SK model, presents unusual properties, such as the characterization of the SG phase by replica-symmetric breaking order parameters[9] organized in a hierarchical structure, defining an ultrametric space. In the presence of an external uniform field (easy axis direction), we have the existence of a phase transition, called by de Almeida–Thouless (AT) line,[10] which separates a high-temperature region where the SG order parameter is unique from a low-temperature one, defined in terms of an infinite number of order parameters.[9] Another exactly solvable SG mean field model was proposed by van Hemmen[11] (VH model). Unlike the SK model, the above model does not depend on the use of the replica trick. The validity of the mean field results for the description of real SG represents a very controversial matter.[12]

The quantum version of the SK Ising spin glass in a transverse field proposed in Ref. 13 was first motivated by the experimental results in mixed-hydrogen-bonded ferroelectrics.[14] Various authors[13,15–32] have considered the Ising SG in a transverse field, with predictions ranging from the destruction of the SG state to an enhancement in the transition temperature with the introduction of quantum fluctuations. Experimentally, in the classical SG phase transition, the ac susceptibility $\chi(w)$ does not diverge at the freezing temperature T_c but merely exhibits a *cusp*. On the other hand, the *nonlinear* susceptibility χ_3 presents a critical singularity at T_c, and has been an indispensable physical parameter accessible in experiments to probe the SG phase transition, with a scaling behavior $\chi_3 \simeq |T-T_c|^{-\gamma}$, γ ranging from 0.9 to 3.8. For the case of quantum SG phase transition, for example in the disordered dipolar quantum Ising magnet $LiHo_xY_{1-x}F_4$ (Ref. 4) in the presence of a transverse field, there exist qualitative differences with the their classical counterpart. In the *high-temperature* (small transverse field) limit (i.e., $T>25$ mK) a divergence in χ_3 at the critical point Ω_c is observed (Ω represents the transverse field), in accordance with the classical SG phase transition, i.e., a critical behavior in the form $\chi_3 \simeq |\Omega-\Omega_c|^{-\gamma}$, is exhibited. However, in the *low-temperature* (high transverse field) limit, the divergence in χ_3 effectively disappears; only a flat maximum is encountered.

There are few studies on the calculation of the nonlinear susceptibility χ_3 in quantum spin glass. Using a perturbative approach[16] in the SK model in a transverse field, χ_3 was obtained as a function of the temperature and the transverse field, whereas near the critical field $\Omega_c(T=0)$ we have the usual scaling form $\chi_3 \simeq |\Omega - \Omega_c|^{-\gamma'}$ with γ' lying between 0.29 and 0.75. The studies on the mean field approximation[24,28] have also found a divergence at $\Omega_c(T=0)$ with $\gamma'=1.0$. It has also been shown that the mean field results[28] for the quantum Ising SG present logarithmic corrections to the power-law behavior of χ_3. In finite dimensionality, the Monte Carlo simulations[30] on a square lattice signal even a stronger divergence for χ_3 at $T=0$ with $\gamma' \simeq 2.8$, close to the $\gamma \simeq 2.9$ for the thermal transition in the three-dimensional Ising model. Many of the calculations of χ_3 have been performed in the static limit, i.e., χ_3 independent of the frequency. Therefore, these works have observed the usual critical behavior $\chi_3 \simeq |\Omega - \Omega_c|^{-\gamma'}$ in the low-temperature regime, in clear contradiction with experimental measurements of the magnetic $LiHo_xY_{1-x}F_4$ (Ref. 4) that shows a flat maximum.

The experimental data in the magnetic system $LiHo_xY_{1-x}F_4$ have shown that sufficient dilution destroys the long-range order,[4] and the disorder and frustration (caused by a competition between the ferromagnetic and antiferromagnetic interactions in a dipole-coupled system) combine to give rise to a SG phase at $x=0.167$ with a transition temperature $T_c \simeq 0.15$ K. They have measured the imaginary component of the dynamic susceptibility $\chi''(w)$ as a function of both w and the strength of the transverse field above and below the SG transition temperature $T_c(\Omega=0)=0.15$ K. The application of the transverse field Ω radically affects the time scale of the Ising system's response. The measurement of the static susceptibility χ_o [or dc susceptibility, that is the $w \to 0$ limit of the real part $\chi'(w)$] presents a finite slope at the zero transverse field with $\partial\chi_o/\partial\Omega|_{\Omega=0}=0$. The theoretical study of the dynamic *nonlinear* susceptibility $\chi_3(w)$ (Ref. 23) in the quantum spherical SG model has been performed exactly to show that the divergence occurs when the frequency approaches the zero-value, but a nonsingular behavior is observed at the critical point $T=0$ for $w \neq 0$.

Some quantum spin glass models have been proposed in the literature, for example, the quantum SK,[15] quantum rotors,[1,20] p-spin in a transverse field,[25] and quantum p-spin spherical[33] models. It is generally found that, in terms of a suitably defined quantum parameter Ω, a critical line $T_c(\Omega)$ in the $T-\Omega$ plane separates the quantum spin glass and the paramagnetic phases. In the case of the quantum p-spin model,[25,30] we have a tricritical point at (T_t, Ω_t) that separates the critical curve $T_c(\Omega)$ in two parts: For $T > T_t$ (high-temperature) the SG phase transition is of second-order, and for $T < T_t$ (low-temperature) we have the first-order phase transition driven by quantum fluctuations. The limit of $p=2$ corresponds to the quantum SK model,[15] and the phase transition is continuous (second-order). For $p \geq 3$ the critical behavior at low temperatures presents a first-order phase transition with a small latent heat, that decreases in the form T^{p-1} (where T is the absolute temperature). Generally, these approximations can be the source of ambiguity at zero temperature where the third law of thermodynamics is usually violated. Another quantum SG model that was recently studied[34] is the generalization of the VH model[11] in the presence of a transverse field (quantum VH model), where the stability limit (phase diagrams) was investigated.

In the past few decades, various types of anisotropies indicate a profound influence on the critical properties of the spin models. The anisotropies due to the crystal-field of the host and the nonmagnetic impurities which affect the spin interaction symmetries are some of the examples. The main models are the Blume-Capel[35] (BC) and Blume-Emery-Griffiths[36] (BEG) models. Besides considering the effects of Ising exchange interactions, the BC model includes a longitudinal crystal field, while the BEG model deals with a biquadratic interaction and a longitudinal crystal field in a Hamiltonian. This longitudinal crystal-field anisotropy has been shown to describe the excitation energy to create the bipolarons for a ferroelectric phase transition in $SrTiO_3$ compound.[37] These classical models have emerged as good candidates for displaying first- or second-order phase transition. A tricritical point and the reentrant behavior are also observed in the phase diagram for the integer spin case. In particular, the BC model is described by the following Hamiltonian:

$$\mathcal{H}_{BC} = -J\sum_{\langle i,j\rangle} S_i^z S_j^z + D\sum_i (S_i^z)^2, \tag{1}$$

where the first sum is over the pairs of nearest-neighbor spins, J is the exchange interaction, D represents the longitudinal crystal field, and S_i^z is the z component of the spin-1 operator at site i. In the classical case, when the positive uniaxial anisotropy $(D>0)$ is large at low temperatures, one obtains a condensation into a nonmagnetic spin phase (or paramagnetic phase P) accompanied by the destruction of the ferromagnetic (F) state, whereas the ferromagnetic phase exists for arbitrary positive values of $D < D_c = zJ/2$ (z is the coordination number). At point $D=D_c$ we have a first-order phase transition between the F and P phases. For $D=0$, model (1), the phase diagram in the $(T-D)$ plane in two and three-dimensional lattices presents a second-order phase transition at high temperatures. Moreover, with the increase of D the critical temperature decreases. At low temperatures, the system presents a first-order phase transition, with a tricritical point (TCP) separating these transitions. The pure BC model (1) has been studied intensively by various methods: *Mean-field approximation* (MFA),[35,38] *effective-field theory* (EFT),[39–42] *renormalization group approach*,[43–45] *series expansion*,[46] *Monte Carlo simulation*,[47] and so on.

An extension of the BC model with random exchange interaction (J_{ij}) has been exactly solved for the infinite-range interaction case. This model is not only simple but is also experimentally accessible. Hence it can be used to describe the thermodynamic properties of the (SG) state. Randomness and frustration are present and in the mean-field limit the equations of state $m=\langle\langle S_i^z\rangle\rangle_c = f(m,q)$ and $q=\langle\langle S_i^z\rangle^2\rangle_c = g(m,q)$ are derived, where $\langle\cdots\rangle_c$ denote the configurational average, m is the magnetization per spin, and q is the SG order parameter per spin. The simple versions of the random BC model have been considered by various authors to describe the SG phase that are described by the VH (Ref. 48) and SK (Ref. 49) models.

On the other hand, the determination of the properties of quantum models is a nontrivial problem due to the noncommutativity of the operators in the Hamiltonian. In particular, the influence of a transverse crystal-field in the BC model (1) can even change the nature of the phase transition because of the quantum effects. The Hamiltonian is given by

$$\mathcal{H} = -J\sum_{\langle i,j\rangle} S_i^z S_j^z + D\sum_i (S_i^z)^2 + D'\sum_i (S_i^x)^2, \qquad (2)$$

where D' is the transverse crystal-field anisotropy parameter. Using the spin identity $(S_i^x)^2+(S_i^y)^2+(S_i^z)^2=S(S+1)$. Equation (2) can be rewritten as

$$\mathcal{H} = -J\sum_{\langle i,j\rangle} S_i^z S_j^z - D_x\sum_i (S_i^x)^2 - D_y\sum_i (S_i^y)^2, \qquad (3)$$

where $D_x=D-D'$ and $D_y=D$. In particular, for $D'=0$ or $D_x=D_y$ the quantum Hamiltonian (3) reduces to the purely classical model (1).

The pure Ising model with biaxial anisotropy given by Eq. (3) has been studied by using the effective-field theory (EFT).[50–54] The appearance of this anisotropy has been demonstrated experimentally by changing the thickness of the nonmagnetic TaN interlayer in FeTaN/TaN/FeTaN sandwiches.[55]

Jiang and Wang[56] have included in the Eq. (3) a transverse magnetic field and the new Hamiltonian is now given by

$$\mathcal{H} = -J\sum_{\langle i,j\rangle} S_i^z S_j^z - D_x\sum_i (S_i^x)^2 - D_y\sum_i (S_i^y)^2 - \Omega\sum_i S_i^x, \qquad (4)$$

where Ω is the transverse field.

The transverse crystal-field and magnetic field parameters in the Hamiltonian present different effects. For example, in the Hamiltonian (4) with $D_x=D_y=0$, Ω destroys the long-range order, where only second-order phase transition is observed in the phase diagram and the system is invariant to the change in the sign of Ω, i.e., $T_c(-\Omega)=T_c(\Omega)$. The critical behavior of the phase diagram in the $T-\Omega$ plane shows a maximum point at $\Omega=0$, with the critical temperature decreasing with the increase in the transverse field and at $T=0$ we have two symmetric quantum phase transitions at $\Omega=\pm\Omega_c$ that are dependent on the topology of the lattice. On the other hand, in the case of the Hamiltonian (4) with $\Omega=D_y=0$, the parameter D_x also destroys the long-range order. However, we have second- and first-order phase transitions in the phase diagram that are dependent on the dimensionality of the lattice and the sign of D_x [i.e., $T_c(-D_x)\neq T_c(D_x)$ for $D_x\neq 0$]. For large values of D_x, positive or negative, the system has no long-range order, while the ordered phase exists for D_x between $D_{1x}<0$ and $D_{2x}>0$.

Results obtained by EFT (Ref. 53) on a simple cubic lattice have shown a second-order phase transition and the critical temperature goes to zero at two symmetric critical transverse crystal-field values $D_{1x}=-D_{2x}$ for $D_y=0$. Moreover, it was observed that with the increase in D_x starting from the negative value, T_c increases from $T_c=0$ at $D_x=D_{1x}$, passes through a maximum at $D_x<0$, and vanishes again at a positive value of $D_x=D_{2x}$. The phase diagram in the $T-D_x$ plane is completely different than that in the $T-D_z$ plane for the Blume-Capel model, where the latter presents first- and second-order phase transitions with presence of a TCP. Another interesting result observed by Xu and Yan[53] in the Hamiltonian (4) with $\Omega=0$ is the presence of a TCP only for $D_y>0$. On the contrary, mean-field solution indicated the presence of a TCP (corresponds to the limit of infinite coordination number, $z\to\infty$) for $D_y=0$ and can be attributed to the presence of long-range interaction.

Previous studies in the Ising model with biaxial anisotropy have concentrated on the pure limit, and did not address the disordered model. In fact, the disordered distribution plays an important role in the spin models, and it may affect the order of the phase transition and lead to some new results. Various works have studied the spin glass Ising model with biaxial anisotropy. The TCP in the quantum anisotropic spin-1 glass Ising model has been investigated.[57] They showed that the disordered model possesses unusual features, manifesting both continuous and first-order phase transitions. This shows that the role of the biaxial crystal field is very important. Yet few works have ever considered a quantum SG Ising model with biaxial anisotropy and transverse magnetic field. At this stage, it is then natural to ask the question as to what would happen if one treats the SG phase by considering a more general model with competing anisotropies. It is clear that some preliminary studies have been made only for some particular cases: (i) For $\Omega=0$ (absence of transverse field) using the SK model;[57] for $\Omega=0$ and $D_x=D_y$ (longitudinal crystal-field) using the VH (Ref. 48) and SK (Ref. 49) models. However, to the best of our knowledge, no attention has been paid to the nature of the phase transition in the more general case of the random long-range exchange interaction (mean-field approach) given by the Hamiltonian (4). This fact has motivated the present investigation, where the quantum SG phase transition is studied by employing the generalized VH model.

The organization of the present paper is as follows. In Sec. II, the quantum VH model and formalism are presented. The detailed numerical results and discussions are presented in Sec. III. Finally, some concluding remarks are given in Sec. IV.

II. GENERAL FORMULATION

The generalization of the classical Mattis spin glass model[58] with competing interactions has been studied by various authors.[11,24,59–62] The study of this generalized Mattis model is very interesting not only in understanding the behavior of those relatively realistic spin glass models but also in the context of the models of neural networks that is known as the Hopfield spin glass.[63]

A. Model

The purpose of this paper is to study the quantum phase transition of the generalized VH model with biaxial anisotropy and transverse field described by the following Hamiltonian

$$\mathcal{H} = -\frac{J_o}{N}\sum_{(i,j)} S_i^z S_j^z - \sum_{(i,j)} J_{ij} S_i^z S_j^z - H\sum_i S_i^z - \Omega\sum_i S_i^x - \sum_i [D_x (S_i^x)^2 + D_y (S_i^y)^2], \tag{5}$$

where (i,j) denotes a sum over all possible pairs of spins, J_o represents a ferromagnetic interaction, H and Ω are the longitudinal and transverse magnetic fields, respectively, D_μ is the transverse crystal field ($\mu = x,y$), S_i^ν is the $\nu(=x,y,z)$ component of a spin operator at site i, and J_{ij} is the spin glass random coupling defined by

$$J_{ij} = \frac{J}{N}(\xi_i \eta_j + \xi_j \eta_i), \tag{6}$$

where ξ_i's and η_i's are independent, identically distributed, random variables with even distribution around zero and a finite variance. We are interested in particular in the $T=0$ limit, where the effect of quantum fluctuations on phase diagram is examined.

In the model (5), the ferromagnetic bonds (J_o) favor a parallel alignment of the spins whereas the antiferromagnetic bonds (random exchange J_{ij}) can favor an antiparallel alignment. The competition of ferromagnetic and antiferromagnetic bonds induce *frustration* to a spin glass model. We restrict ourselves to the case of two different distributions, the discrete (or *bimodal distribution*) is given by

$$\mathcal{P}_B(x_i) = \frac{1}{2}[\delta(x_i - 1) + \delta(x_i + 1)], \tag{7}$$

and the continuous (or *Gaussian distribution*) given by

$$\mathcal{P}_G(x_i) = \frac{1}{\sqrt{2\pi}} e^{-x_i^2/2}, \tag{8}$$

where $x_i = \xi_i$ or η_i.

In order to study theoretically the thermal properties of the Hamiltonian (5), we have to calculate the partition function

$$\mathcal{Z} = \mathrm{Tr}\, e^{-\beta\mathcal{H}} = \sum_\mu \langle \mu | e^{-\beta\mathcal{H}} | \mu \rangle, \tag{9}$$

for the orthogonal complete set of states $|\mu\rangle$.

B. Calculations

Some obvious identities should be satisfied that are important to calculate the partition function $\mathcal{Z}$, such as

$$\sum_{(i,j)} S_i^z S_j^z = \frac{1}{2}\left[\left(\sum_i S_i^z\right)^2 - \sum_i (S_i^z)^2\right] \tag{10}$$

and

$$\sum_{(i,j)} (\xi_i \eta_j + \xi_j \eta_i) S_i^z S_j^z = \frac{1}{2}\left\{\left[\sum_i (\xi_i + \eta_i) S_i^z\right]^2 - \left(\sum_i \xi_i S_i^z\right)^2 - \left(\sum_i \eta_i S_i^z\right)^2 - 2\sum_i \xi_i \eta_i (S_i^z)^2\right\}. \tag{11}$$

Using the identities (10) and (11), the Hamiltonian (5) can be rewritten as

$$\mathcal{H} = -\frac{J_o}{2N}\left(\sum_i S_i^z\right)^2 - \frac{J}{2N}\left[\sum_i (\xi_i + \eta_i) S_i^z\right]^2 + \frac{J}{2N}\left(\sum_i \xi_i S_i^z\right)^2 + \frac{J}{2N}\left(\sum_i \eta_i S_i^z\right)^2 - \sum_i \mathcal{A}_i, \tag{12}$$

with

$$\mathcal{A}_i = \sum_{\nu=x,y,z} [H_i^\nu S_i^\nu + D_i^\nu (S_i^z)^2], \tag{13}$$

where $H_i^x = \Omega$, $H_i^y = 0$, $H_i^z = H$, $D_i^x = D_x$, $D_i^y = D_y$, and $D_i^z = (J/2N)(\alpha + 2\xi_i \eta_i)$ $(\alpha = J_o/J)$.

Many methods for studying the quantum spin systems are based on the Suzuki-Trotter formula.[64] According to this formula, we can decompose an exponential operator instead of working with the original expression $e^{-\beta\mathcal{H}}$. By this decomposition method, we can obtain more accurate approximations to the original operator. We consider the exponential operator e^{A+B}, where A and B are noncommutable operators. In many cases, it is difficult to diagonalize the sum of the operators, $A+B$. If it is practically possible to diagonalize each A and B, then the simplest correction term in first order is[65]

$$e^{A+B} \simeq e^A e^B. \tag{14}$$

Now, using the approximate decomposition in first order (14) we can express the partition function as

$$\mathcal{Z} = \mathrm{Tr}\left\{ e^{(K_o/2N)\left(\sum_i S_i^z\right)^2} e^{(K/2N)\left[\sum_i (\xi_i + \eta_i) S_i^z\right]^2} e^{-(K/2N)\left(\sum_i \xi_i S_i^z\right)^2} \times e^{-(K/2N)\left(\sum_i \eta_i S_i^z\right)^2} \prod_{i=1}^N e^{\beta\mathcal{A}_i} \right\}, \tag{15}$$

where $K_o = \beta J_o$ and $K = \beta J$.

The quadratic terms in Eq. (15) can be rewritten by using the Gaussian identity

$$e^{\alpha\sigma^2} = \frac{1}{\sqrt{2\pi}}\int_{-\infty}^{\infty} dx\, e^{-x^2/2 + \sqrt{2\alpha}\sigma x}. \tag{16}$$

Using this identity, Eq. (15) is rewritten as follows

$$\mathcal{Z} = \frac{N^2}{4\pi^2}\int_{-\infty}^{\infty} dx \int_{-\infty}^{\infty} dy \int_{-\infty}^{\infty} dz \int_{-\infty}^{\infty} dw \times e^{-(N/2)(x^2+y^2+z^2+w^2) + N \ln \Phi(x,y,z,w)}, \tag{17}$$

with

$$\Phi(x,y,z,w) = \mathrm{Tr}\{e^{L_1 S^z + L_2 S^x + L_3 (S^x)^2 + L_4 (S^y)^2 + L_5 (S^z)^2}\}, \tag{18}$$

where

$$L_1 = \sqrt{K_o}x + \sqrt{K}[(\xi + \eta)y + i(\xi z + \eta w)] + L, \qquad (19)$$

$$L_2 = \beta\Omega, \qquad (20)$$

$$L_3 = \beta D_x, \qquad (21)$$

$$L_4 = \beta D_y, \qquad (22)$$

and

$$L_5 = \frac{K}{2N}(\alpha + 2\xi\eta), \qquad (23)$$

where $i=\sqrt{-1}$ is the pure complex number and $\alpha=J_o/J$.

In the present model only a quenched system is considered where the free energy rather than the logarithm of the partition function is to be averaged. Therefore, the free energy per spin is given by the following expression:

$$f \equiv -\frac{\beta F}{N} = \left\langle \frac{\ln \mathcal{Z}}{N} \right\rangle_c = \int_{-\infty}^{\infty} d\eta \int_{-\infty}^{\infty} d\xi\, \mathcal{P}(\eta)\mathcal{P}(\xi)\frac{\ln \mathcal{Z}}{N}. \qquad (24)$$

Using the steepest-descent method Eq. (17) can be written in the thermodynamic limit ($N\to\infty$) as

$$f \equiv \left\langle \lim_{N\to\infty}\left\{\frac{\ln \mathcal{Z}}{N}\right\}\right\rangle_c = -\frac{(x^{*2} + y^{*2} + z^{*2} + w^{*2})}{2} + \langle \ln \Phi(x^*,y^*,z^*,w^*)\rangle_c. \qquad (25)$$

The saddle-point condition becomes

$$\left(\frac{\partial f}{\partial x}\right)_* = 0 \to x^* = \sqrt{K_o}m,$$

$$\left(\frac{\partial f}{\partial y}\right)_* = 0 \to y^* = \sqrt{K}(q_1 + q_2),$$

$$\left(\frac{\partial f}{\partial z}\right)_* = 0 \to z^* = i\sqrt{K}q_1,$$

$$\left(\frac{\partial f}{\partial w}\right)_* = 0 \to w^* = i\sqrt{K}q_2, \qquad (26)$$

where the asterisk represents the value at a saddle point, and

$$m = \left\langle\left\langle \frac{1}{N}\sum_i S_i^z \right\rangle\right\rangle_c, \qquad (27)$$

$$q_1 = \left\langle\left\langle \frac{1}{N}\sum_i \xi_i S_i^z \right\rangle\right\rangle_c, \qquad (28)$$

and

$$q_2 = \left\langle\left\langle \frac{1}{N}\sum_i \eta_i S_i^z \right\rangle\right\rangle_c, \qquad (29)$$

where m is the average magnetization per spin and q_1 and q_2 are the average SG order parameters per spin, defined by van Hemmen.[11] At the saddle point $P=(x^*,y^*,z^*,w^*)$, Eq. (25) becomes

$$f(m,q_1,q_2) = -\frac{(K_o m^2 + 2K_{q_1 q_2})}{2} + \langle \ln \Phi(x^*,y^*,z^*,w^*)\rangle_c, \qquad (30)$$

with

$$\Phi(x^*,y^*,z^*,w^*) = \mathrm{Tr}\, e^{\mathcal{B}} \equiv \mathrm{Tr}\{e^{hS^z + \beta\Omega S^x + \beta D_x (S^x)^2 + \beta D_y (S^y)^2}\}, \qquad (31)$$

where $h=K_o m + K(\xi q_2 + \eta q_1) + \beta H$, and in the $N\to\infty$ limit the parameter L_5 of Eq. (23) is zero.

For spin $S=1$, in S^2 and S^z representation $\mathcal{B}$ can be written in the form of 3×3 matrix as

$$\mathcal{B} = \begin{bmatrix} h + L^+ & a & L^- \\ a & 2L^+ & a \\ L^- & a & -h + L^+ \end{bmatrix}, \qquad (32)$$

where $\mathcal{L}^{\pm}=\beta(D_x \pm D_y)/2$ and $a=\beta\Omega/\sqrt{2}$. This form of $\mathcal{B}$ can readily be diagonalized and its eigenvalues found. Then the three eigenvalues are

$$\lambda_1 = -a_1/3 + 2\sqrt{-Q}\cos\frac{\theta}{3},$$

$$\lambda_2 = -a_1/3 + 2\sqrt{-Q}\cos\left(\frac{\theta + 2\pi}{3}\right),$$

$$\lambda_3 = -a_1/3 + 2\sqrt{-Q}\cos\left(\frac{\theta + 4\pi}{3}\right), \qquad (33)$$

with

$$\theta = \arccos(-R/\sqrt{-Q^3}), \qquad (34)$$

$$R = (9a_1 a_2 - 27a_3 - 2a_1^3)/54, \qquad (35)$$

$$Q = (3a_2 - a_1^2)/9, \qquad (36)$$

$$a_1 = -4L^+, \qquad (37)$$

$$a_2 = 5(L^+)^2 - h^2 - (L^-)^2 - 2a^2, \qquad (38)$$

and

$$a_3 = -2(L^+)^3 + 2L^+[(L^-)^2 + h^2] - 2a^2(L^- - L^+). \qquad (39)$$

Then Eq. (31) can be written as

$$\Phi(T,H,D_x,D_y,\Omega) = \mathrm{Tr}\{e^{\mathcal{B}}\} = \sum_{r=1}^{3} e^{\lambda_r}, \qquad (40)$$

where the eigenvalues $\{\lambda_1,\lambda_2,\lambda_3\}$ are given in Eq. (33).

C. Free energy and equations of state

Substituting Eq. (40) in Eq. (30) we have the free energy given by

$$f(m,q) = -\frac{(K_o m^2 + 2Kq^2)}{2} + \left\langle \ln \sum_{r=1}^{3} e^{\lambda_r} \right\rangle_c , \quad (41)$$

whose minimum corresponds always to $q_1 = q_2 = q$, m where q is given by the self-consistent equations

$$m = \int_{-\infty}^{\infty} d\eta \int_{-\infty}^{\infty} d\xi\, \mathcal{P}(\eta)\mathcal{P}(\xi)\left(\frac{\partial \ln \Phi}{\partial L}\right)_{H=0} \quad (42)$$

and

$$q = \frac{1}{2}\int_{-\infty}^{\infty} d\eta \int_{-\infty}^{\infty} d\xi (\xi + \eta)\mathcal{P}(\eta)\mathcal{P}(\xi)\left(\frac{\partial \ln \Phi}{\partial L}\right)_{H=0}, \quad (43)$$

where $\mathcal{P}(x)$ is the probability distribution given by Eq. (7), for the bimodal distribution case, or by Eq. (8), for the Gaussian distribution case. From the above equations it follows that for $\Omega=0$ and $D_x = D_y$ (longitudinal crystal field) one recovers the results of de Almeida and Moreira.[48]

III. RESULTS AND DISCUSSION

All the results presented in this section are obtained from the numerical solutions of Eqs. (41)–(43). To study the phase diagram, we define the dimensionless parameters: $T \equiv (\beta J)^{-1}$, $\alpha \equiv J_o/J$, $d_x = D_x/J$, $d_y = D_y/J$, and $\delta = \Omega/J$. We restrict the study for the case of $\alpha = 0$, where the interactions are random in sign and the ordering is of SG type $(m=0, q \neq 0)$.

The second-order phase transition occurs with the breakdown of the SG order parameter q. So the phase transition boundaries of the SG phase are determined from the zero value of the coefficient of the second-order term in Eq. (41) when the free energy is expanded in terms of q. The Landau free energy expansion is given by

$$F(q) \simeq a_2 q^2 + a_4 q^4 + a_6 q^6 + \dots , \quad (44)$$

where the coefficients $a_n = (1/n!)(\partial^n f/\partial q^n)_{q=0}$ are functions of the parameters d_x, d_y, and δ. The coordinates of the TCP are determined by $a_2 = a_4 = 0$ and $a_6 < 0$ and the second-order transition by $a_2 = 0$ and $a_4 > 0$. Some authors[51,56] have used the condition $a_2 = 0$ and $a_4 < 0$ *erroneously* to determine the first-order line, but this condition corresponds to the *unstable* solution of the system.

For $J_o = 0$, ferromagnetic (F) phase is not expected. However, there is a transition temperature from the SG to the paramagnetic (P) phase that is dependent on the parameters Ω, D_x, and D_y. The phase transition between the SG $(m=0, q \neq 0)$ and $P(m=0, q=0)$ phases is determined by equaling the free energies of the two phases, i.e., $f_P(0,0) = f_{SG}(0,q)$ and the SG order parameter q is given by Eq. (43). Simultaneously solving these expressions we obtain the freezing temperature T_c as a function of Ω, D_x, and D_y. For second-order (continuous) phase transition we find $q=0$, while for the first-order phase transition $q \neq 0$ and this finite value corresponds to the discontinuity of the SG order parameter at $T = T_c$. When $J_o \neq 0$, a F phase $(m \neq 0, q=0)$ exists in addition to the SG and P phases. In the case of the bimodal distribution given by Eq. (7), we also have the mixed phase (M) characterized by $(m \neq 0, q \neq 0)$.

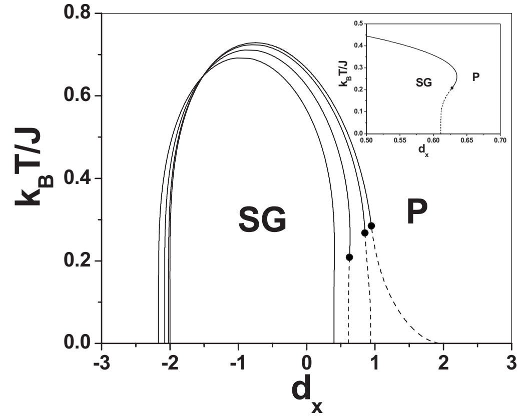

FIG. 1. Phase diagram in the $T - d_x$ plane for the VH biaxial model with $d_y = 0$ and different values of transverse field $\delta(=0, 0.2, 0.4, 0.6)$ in decreasing order. The continuous (dashed) lines correspond to the second (first)-order phase transition line. The TCP is made by a black circle. The inset shows the region of the reentrant behavior at low temperature for $\delta = 0.4$.

First, let us examine the variation of the reduced transition temperature with the transverse crystal field d_x for $d_y = 0$ and different values of $\delta(=0, 0.2, 0.4, 0.6)$. The results are depicted in Fig. 1, where we use the bimodal distribution. The choice of the bimodal and the Gaussian has been based on including two very different kinds of distribution. Please note that the differences between the bimodal (discrete) and the Gaussian (continuous) distributions are qualitatively high in all respects. Hence, when the Gaussian and the bimodal give similar results, we believe that a trimodal (discrete) distribution, for example, should not change our results qualitatively. The solid lines represent the critical temperature, dashed lines the first-order transition temperature, and the black circles the TCP. For $\delta = 0$ and negative values of d_x, the critical temperature increases from $T_c = 0$ at $(d_x)_{1c} = -2.0$ with the increase of d_x, passes through a maximum at $d_x \simeq -0.80$, and then decreases rapidly to a TCP for positive values of d_x. Above TCP and for large values of d_x we have a first-order phase transition line that decreases and T_c vanishes again at a positive $(d_x)_{2c} = 2.0$ value. In the present work, the SG transition temperature goes to zero at the two values of the symmetric transversal crystal field $(d_x)_{1c} = -2.0$ (*quantum critical point*) and $(d_x)_{2c} = 2.0$ (*quantum first-order point*). The stability limit of the SG phase presented in Fig. 1 for $\delta = 0$ and $d_y = 0$ is different than that found on a lattice with finite coordination number $(z < \infty)$ by using EFT in the pure Ising model,[53] where only second-order phase transition was found. The inversion point in the $T - d_x$ plane in Fig. 1 can be understood considering the behavior of the free energy with the three parameters δ, d_x, and T. We see that when $d_x > 0$ the tendency of the minimum of the free energy is to become more and more negative as we increase d_x, T, or the magnetic field. But when we are in the negative values of d_x we ob-

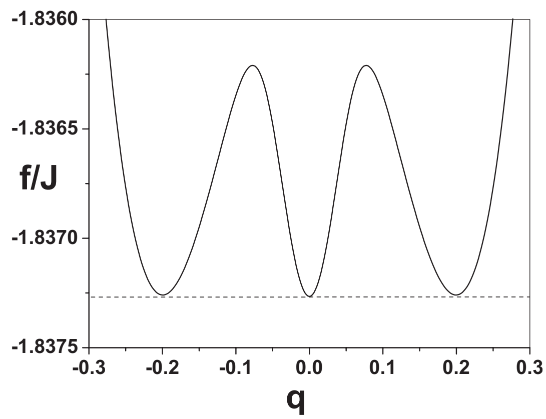

FIG. 2. Behavior of free energy as a function of the SG parameter q for the VH biaxial model with $k_BT/J=0.05$, $\delta=0$, and $d_x=1.94$.

serve that the free energy behaves differently with three parameters. While the minimum of the free energy decreases with the increase of T and field, it increases with the decrease in d_x. Thus the inversion occurs. Moreover, we observe that the Hamiltonian is not symmetric with the change from $d_x \to -d_x$. When the temperature is high we see that still the temperature alone dominates but after $d_x \leq -1.5$, d_x dominates and the inversion occurs.

In order to illustrate the first-order transition behavior in the phase diagram in Fig. 1, we present in Fig. 2 the thermodynamical behavior of the free energy $f(q)$ as a function of the order parameter q. We chose the point $k_BT_c/J=0.05$ and $d_x=1.94$ from Fig. 1 for this analysis. Three minimum points are observed ($q=0, q=\pm 0.20$), where $\Delta q=0.20$ corresponds to the discontinuity of the SG order parameter q in this point of first-order phase transition.

Increasing the transverse field δ, the phase diagram (Fig. 1) has the same topology as that for $\delta=0$, but the TCP disappears when δ is larger than a critical value, $\delta_c=0.501$. The same qualitative results are obtained by using Gaussian distribution; therefore, we will omit the results here. Reentrant phase transition can be seen explicitly for $\delta=0.40$ at low temperatures. The inset in Fig. 1 shows this reentrant behavior. The origin of this reentrance is not so clear, but may be attributed to the competitive quantum effects due to the transverse crystal field and transverse magnetic field (i.e., parameters δ and d_x), where the two effects do not affect in the same manner. The transition in which the transverse crystal field dominates has the tendency to be first order, while the transverse field tends to make it second order. So, when the temperature is lowered from above, the transition is more characteristic of the transverse field. If the temperature is lowered further, the crystal field contributes mainly and the reentrance to the disorder phase may take place. For the parameter d_y in the range $0 \leq d_y < 2$, we have the same qualitative phase diagram in the $T-d_x$ plane with presence of first-order and second-order phase transitions, reentrance and TCP that are dependents of the value of δ. The maximum value of T_c decreases as d_y and δ increases.

In Fig. 3 we present the phase diagram for $\delta=0$ and different values of $d_y(=0,0.1,0.5,1.0) \geq 0$. On the other hand,

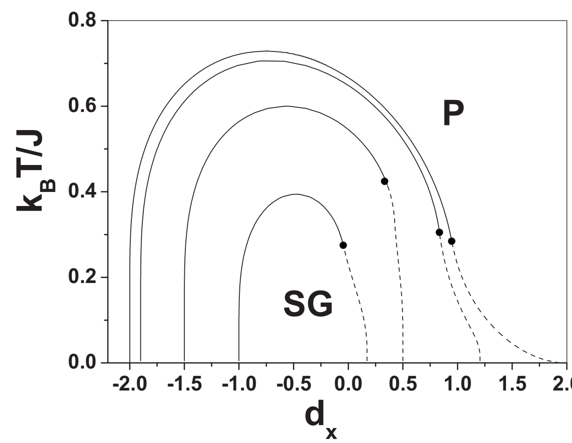

FIG. 3. Phase diagram in the $T-d_x$ plane for the VH biaxial model with $\delta=0$ and different values of transverse crystal-field $d_y(=0,0.1,0.5,1)$ in decreasing order. The continuous (dashed) lines correspond to the second (first)-order phase transition line. The TCP is made by a black circle.

for $d_y<0$ the TCP is absent in all critical lines. The critical temperature goes to zero, for two antisymmetric values: d_{x1} and d_{x2}. Our results are qualitatively similar to that obtained by EFT (Ref. 53) calculations on a simple cubic lattice ($z=6$), except for $d_y=0$ (and $\delta=0$) where we observe a TCP. An extension of the calculations of Xu and Yan[53] using EFT, to investigate the tricritical behavior as a function of the coordination number (z) has been discussed by de Sousa.[66] For $z \geq 7$ a TCP appears in the phase diagram for $D_y=0$, where the tricritical temperature (tricritical transverse crystal-field parameter) increases (decreases) as z increases. Moreover, when $z \to \infty$ the results tend to MFA values $(k_BT/zJ)_{\text{TCP}}=0.2845$ and $(D_x/zJ)_{\text{TCP}}=0.9471$.

We can also show the phase diagram in the $T-d_y$ plane, but the results are entirely the same as those of Figs. 1–3 because the x axis and the y axis are the two equivalent axes relative to the z axis. Therefore, the effects of the two transverse crystal-field parameters are all equivalent.

We study the ground-state behavior of the present model by taking into account the zero temperature limit ($T=0$). To illustrate, we choose $\delta=0$ and obtain the phase diagram in the d_x-d_y plane in Fig. 4. From the figure we observe that when $d_x<0$ and $d_x \geq 0$ we have a second-order (continuous line) and first-order (dashed line) quantum phase transition, respectively. The values of d_x corresponding to $d_y=0$ are symmetric ($d_x=-2.0$ and 2.0). Moreover, in this region we have a SG phase.

In order to investigate the influence of the transverse field, we choose $d_y=0$ to obtain the phase diagram in the $d_x-\delta$ plane at $T=0$. In Fig. 5, we plot the above phase diagram for $d_x<-2.0$ where the SG phase exists between two quantum critical points, δ_{1c} and δ_{2c}, corresponding to a reentrant behavior of the order parameter q as a function of the transverse field δ. For $-2.0<d_x<(d_x)_{\text{TCP}}$ we have only one quantum critical point, where $[(d_x)_{\text{TCP}}=0.498,\ \delta_{\text{TCP}}=0.501]$ corresponds to the coordinates of the TCP. Although there exists no TCP in the negative direction of d_x, we observe that in the positive direction of d_x the TCP exists for $d_y \geq 0$. The

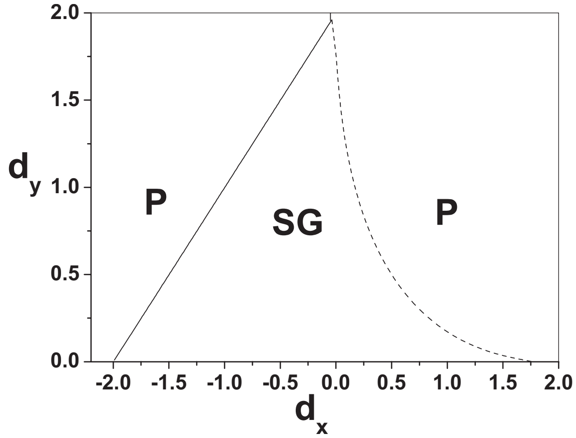

FIG. 4. Ground-state phase diagram in the $d_x - d_y$ plane for the VH biaxial model with $\delta=0$. The continuous (dashed) line corresponds to the second (first)-order phase transition line.

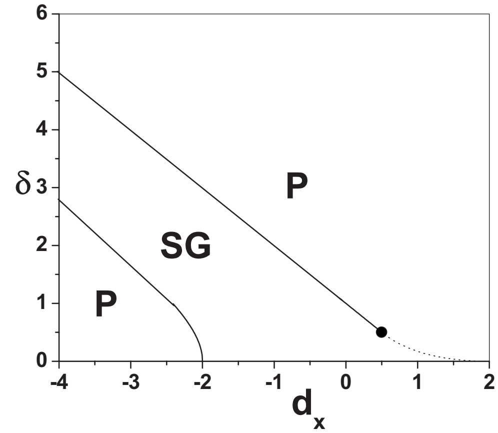

FIG. 5. Ground-state phase diagram in the $d_x - \delta$ plane for the VH biaxial model with $d_y=0$. The continuous (dashed) line corresponds to the second (first)-order phase transition line.

TCP is suppressed as d_y decreases. The second-order transition lines do not touch the d_x axis for all $d_y < 0$.

IV. CONCLUSIONS

In summary, we have studied the phase diagram of the quantum VH model in the presence of a biaxial crystal-field anisotropy and a transverse field. The general formulation for the free energy and order parameter of the model are derived. Unlike the pure model for a simple cubic lattice, we observe the disappearance of TCP for $d_y=0$ and $\delta > 0.501$. In the former case EFT predicts a tricritical behavior for $\delta=0$. Results obtained by de Sousa[66] using EFT have indicated the presence of a TCP when the coordination number is $z > 7$. In the absence of transverse field ($\delta=0$) and $d_y < 0$ only second-order phase transition has been predicted, while for $d_y \geq 0$ a TCP is observed. For the same values of the parameters of the model a reentrant behavior is observed. In particular, for $\delta=0.4$ and $d_y=0$ two transition temperature are found in the range $0.61 < d_x < 0.64$. Finally, it is evident that the present quantum model is not yet sufficiently close to real spin-glass systems.

ACKNOWLEDGMENTS

This work was partially supported by CNPq and FAPEAM (Brazilian agencies).

[1] Subir Sachdev, *Quantum Phase Transitions* (Cambridge University Press, Cambridge, UK, 2001).
[2] M. A. Continentino, *Quantum Scaling in Many Body Systems* (World Scientific, Singapore, 2001), and references therein.
[3] B. K. Chakrabarti, A. Dutta, and P. Sen, *Quantum Ising Phases and Transitions in Transverse Ising Models* (Springer-Verlag, Berlin, 1996).
[4] W. Wu, B. Bitko, T. F. Rosenbaum, and G. Aeppli, Phys. Rev. Lett. **71**, 1919 (1993).
[5] V. Pellegrini, A. Pinczuk, B. S. Dennis, A. S. Plaut, L. N. Pfeiffer, and K. W. West, Science **281**, 799 (1998).
[6] A. Scröder, G. Aeppli, E. Bucher, R. Ramazashvil, and P. Coleman, Phys. Rev. Lett. **80**, 5623 (1998).
[7] E. Manousakis, Rev. Mod. Phys. **63**, 1 (1991).
[8] D. Sherrington and S. Kirkpatrickm, Phys. Rev. Lett. **35**, 1792 (1975).
[9] G. Parisi, Phys. Rev. Lett. **43**, 1754 (1979); **50**, 1946 (1975); M. Mézard, G. Parisi, N. Sourlas, G. Toulouse, and M. A. Virasoro, Phys. Rev. Lett. **52**, 1156 (1984); J. Phys. (Paris) **45**, 843 (1984).
[10] J. R. de Almeida and D. L. Thouless, J. Phys. A **11**, 983 (1978).
[11] J. L. van Hemmen, Phys. Rev. Lett. **49**, 409 (1982).
[12] C. M. Newman and D. L. Stein, Phys. Rev. Lett. **76**, 515 (1996); E. Marinari, G. Parisi, J. Ruiz-Lorenzo, and F. Ritart, Phys. Rev. Lett. **76**, 843 (1996).
[13] T. K. Kopec, K. D. Usadel, and G. Büttner, Phys. Rev. B **39**, 12418 (1989).
[14] E. Courtens, Phys. Rev. Lett. **52**, 69 (1984); E. Courtens, F. Huard, and R. Vacher, Phys. Rev. Lett. **55**, 722 (1985).
[15] A. Bray and M. A. Moore, J. Phys. C **13**, L655 (1980).
[16] H. Ishii and T. Yamamoto, J. Phys. C **18**, 6225 (1985); **18**, 6053 (1985).
[17] D. Thirumalari, Q. Li, and T. R. Kirkpatrick, J. Phys. A **22**, 3339 (1989).
[18] G. Büttner and K. D. Usadel, Phys. Rev. B **41**, 428 (1990).
[19] Y. Y. Goldschmidt and P. Y. Lai, Phys. Rev. Lett. **64**, 2467 (1990).
[20] T. Yokota, Phys. Lett. A **125**, 482 (1987).
[21] Yu-Quiang Ma and Z. Y. Li, Phys. Lett. A **145**, 19 (1990); **148**, 134 (1990).
[22] P. Ray and B. K. Chakrabarti, Phys. Rev. B **39**, 11828 (1989).
[23] T. K. Kopec, Phys. Rev. Lett. **79**, 4266 (1997); Phys. Rev. B **50**, 9963 (1994).
[24] M. S. Li, K. Walasek, and M. Cieplak, Phys. Rev. B **56**, 11715 (1997).
[25] T. M. Nieuwenhuizen and F. Ritort, Physica A **250**, 8 (1998).

[26] T. K. Kopec and R. Pirc, Phys. Rev. B **55**, 5623 (1997); T. K. Kopec and K. D. Usadel, Phys. Rev. Lett. **78**, 1988 (1997).
[27] Y. Banerjee and S. Dattagupta, Phys. Rev. B **50**, 9942 (1994).
[28] J. Ye, S. Sachdev, and N. Read, Phys. Rev. Lett. **70**, 4011 (1993); S. Sachdev and J. Ye, Phys. Rev. Lett. **70**, 3339 (1993); N. Read, S. Sachdev, and J. Ye, Phys. Rev. B **52**, 384 (1995).
[29] R. Pirc, P. Prelovsek, and B. Tadic, Solid State Commun. **64**, 137 (1987).
[30] H. Rieger and A. P. Young, Phys. Rev. Lett. **72**, 4141 (1994); M. Guo, R. N. Bhata, and D. Huse, Phys. Rev. Lett. **72**, 4137 (1994).
[31] M. A. Continentino, B. Boechat, and R. R. dos Santos, Phys. Rev. B **50**, 13528 (1994).
[32] W. Wu, B. Ellman, T. F. Rosenbaum, G. Aeppli, and D. H. Reich, Phys. Rev. Lett. **67**, 2076 (1991).
[33] L. F. Cugliandolo, D. R. Grempel, and C. A. da Silva Santos, Phys. Rev. Lett. **85**, 2589 (2000); Phys. Rev. B **64**, 014403 (2001).
[34] J. Roberto Viana, Yamilles Nogueira, and J. Ricardo de Sousa, Phys. Rev. B **66**, 113307 (2002); Phys. Lett. A **311**, 480 (2003).
[35] M. Blume, Phys. Rev. **141**, 517 (1966); H. W. Capel, Physica (Amsterdam) **32**, 966 (1966).
[36] M. Blume, V. J. Emery, and R. B. Griffiths, Phys. Rev. A **4**, 1071 (1971).
[37] Y. Yamada, N. Todoroki, and S. Miyashita, Phys. Rev. B **69**, 024103 (2004).
[38] M. Kaufman and M. Kanner, Phys. Rev. B **42**, 2378 (1990).
[39] A. F. Siqueira and I. P. Fittipaldi, Physica A **138**, 592 (1986).
[40] J. W. Tucker, J. Magn. Magn. Mater. **183**, 299 (1998).
[41] T. Kaneyoshi, Phys. Rev. B **34**, 7866 (1986); J. Phys. C **19**, L557 (1986).
[42] H. P. Dong and S. L. Yan, J. Magn. Magn. Mater. **308**, 90 (2007), and references therein.
[43] N. S. Branco, Phys. Rev. B **60**, 1033 (1999); N. S. Branco and B. M. Boechat, Phys. Rev. B **56**, 11673 (1997).
[44] H. Dickinson and J. Yeomans, J. Phys. C **16**, L345 (1983).
[45] J. A. Plascak and D. P. Lara, Mod. Phys. Lett. A **10**, 1996 (1996).
[46] Z. Onyskiewicz, P. Sweykowski, G. I. Georgiev, and M. P. Sandalski, Acta Phys. Pol. A **59**, 379 (1981).
[47] J. A. Plascak, D. P. Lara, S. J. Ferreira, and O. F. A. Bonfim, J. Magn. Magn. Mater. **177**, 163 (1998).
[48] J. R. L. de Almeida and F. G. B. Moreira, Z. Phys. B: Condens. Matter **63**, 365 (1982).
[49] E. J. S. Lage and J. R. L. de Almeida, J. Phys. C **10**, 1187 (1982); P. J. Mottishaw and D. Sherrington, J. Phys. C **18**, 5201 (1985); F. A. Costa, C. S. O. Yokoi, and S. R. A. Salinas, J. Phys. A **27**, 3365 (1994).
[50] J. Oitmaa and A. M. A. V. Brasch, Phys. Rev. B **67**, 172402 (2003).
[51] Q. Zhang, G. Z. Wei, and Y. Q. Liang, J. Magn. Magn. Mater. **253**, 45 (2002).
[52] W. Jiang, G. Z. Wei, and Q. Zhang, Physica A **329**, 161 (2003).
[53] L. Xu and S. L. Yan, Solid State Commun. **142**, 159 (2007).
[54] J. Wei, W. Xi-Kum, and Z. Qiang, Chin. Phys. **15**, 1009 (2006).
[55] H. B. Nie, C. K. Ong, J. P. Wang, and Z. W. Li, J. Appl. Phys. **93**, 7252 (2003).
[56] W. Jiang and S. Wang, Physica A **341**, 333 (2004). See also M. Boughrara, M. Kerouad, M. Saber, and D. Baldomir, Chin. J. Phys. (Taipei) **45**, 75 (2007), and references therein.
[57] Z. Domanski and T. K. Kopec, J. Phys.: Condens. Matter **12**, 5727 (2000).
[58] D. C. Mattis, Phys. Lett. **56A**, 421 (1976).
[59] J. P. Provost and G. Vallee, Phys. Rev. Lett. **50**, 598 (1983).
[60] Yamilles Nogueira, J. Roberto Viana, and J. Ricardo de Sousa, Braz. J. Phys. **37**, 331 (2007).
[61] P. T. Muzy, A. P. Vieira, and S. R. Salinas, Physica A **359**, 469 (2006).
[62] S. G. Magalhães, F. M. Zimmer, P. R. Krebs, and B. Coqblin, Phys. Rev. B **74**, 014427 (2006).
[63] J. J. Hopfield, Proc. Natl. Acad. Sci. U.S.A. **79**, 2554 (1982); **81**, 3088 (1984).
[64] H. F. Trotter, Proc. Am. Math. Soc. **10**, 545 (1959); M. Suzuki, Commun. Math. Phys. **51**, 183 (1976); see also M. Suzuki, *Quantum Monte Carlo Methods* (Springer, Berlin, 1986).
[65] M. Suzuki, *Exponential Product Formulas and Quantum Analysis* (University of Tokyo, Tokyo, 1996).
[66] J. Ricardo de Sousa (private communication).